Defining a quantum active particle using a non-unitary quantum walk: Supplementary Mateiral

Manami Yamagishi,[1,2,*] Naomichi Hatano,[3,†] and Hideaki Obuse[4,3,‡]

[1]*Department of Physics, the University of Tokyo, 5-1-5 Kashiwanoha, Kashiwa, Chiba 277-8574, Japan*
[2]*Theoretical Quantum Physics Laboratory, RIKEN, 2-1 Hirosawa, Wako, Saitama 351-0198, Japan*
[3]*Institute of Industrial Science, the University of Tokyo, 5-1-5 Kashiwanoha, Kashiwa, Chiba 277-8574, Japan*
[4]*Department of Applied Physics, Hokkaido University, Kita13jo Nishi8cho, Kita, Sapporo, Hokkaido 060-8628, Japan*

(Dated: July 24, 2024)

S-I. REVIEW OF QUANTUM WALKS IN ONE DIMENSION AND HIGHER DIMENSIONS

A. One-dimensional quantum walks

The quantum walk was first proposed in one dimension [1]. In addition to the spatial degree of freedom $|x\rangle$, we let each lattice point have an internal degree of freedom of two states $|\mathrm{L}\rangle$ and $|\mathrm{R}\rangle$. The entire state space is thereby spanned by $|x\rangle \otimes |\mathrm{L}\rangle$ and $|x\rangle \otimes |\mathrm{R}\rangle$.

The shift operator $\tilde{S}$ is defined to move the spatial part of the state according to the internal degree of freedom:

$$\tilde{S} := \sum_x [|x-a\rangle\langle x| \otimes |\mathrm{L}\rangle\langle \mathrm{L}| + |x+a\rangle\langle x| \otimes |\mathrm{R}\rangle\langle \mathrm{R}|], \tag{S1}$$

where a is the lattice constant. In other words, the wave function of the component $|\mathrm{L}\rangle$ is shifted to the left by one lattice constant, while that of $|\mathrm{R}\rangle$ is shifted to the right by one lattice constant. (Note that throughout the paper, we put the lattice constant a to unity, for simplicity.) If we kept operating the shift operator only, the left-going component would keep moving left, while the right-going component would keep moving right, without any interaction between them. We hence additionally introduce the coin operator

$$\tilde{C} := \sum_x [|x\rangle\langle x| \otimes u], \tag{S2}$$

where u is a 2×2 unitary matrix that shuffles the left-going and right-going components at each lattice point. Throughout the present paper we use the following specific form for the unitary u:

$$u = \begin{pmatrix} \cos\theta & -\sin\theta \\ \sin\theta & \cos\theta \end{pmatrix}. \tag{S3}$$

Taking the initial state

$$|\psi(0)\rangle = \frac{1}{\sqrt{2}} |0\rangle \otimes (|\mathrm{L}\rangle + \mathrm{i}\,|\mathrm{R}\rangle), \tag{S4}$$

for example, and applying the shift and coin operators repeatedly as in

$$|\psi(T)\rangle = \left(\tilde{S}\tilde{C}\right)^T |\psi(0)\rangle\,, \tag{S5}$$

we observe the probability distribution $\langle\psi(T)|\psi(T)\rangle$ in Fig. S1(a).

We can understand this probability distribution as follows. In classical random walks, the walker that starts from the origin takes various paths stochastically. Each path has its own positive probability. Since there are more paths around the starting point, the probability accumulates higher around there. In quantum walks, on the other hand, each path has its own amplitude, which is generally complex. Although there are more paths around the starting point, they interfere with each other because of their random phases instead of the probability accumulation. This interference decreases the probability around the origin. Since the number of paths is small near the right and left wave fronts, the interference is weaker, and hence the probability has peaks there.

* manami@iis.u-tokyo.ac.jp
† hatano@iis.u-tokyo.ac.jp
‡ hideaki.obuse@eng.hokudai.ac.jp

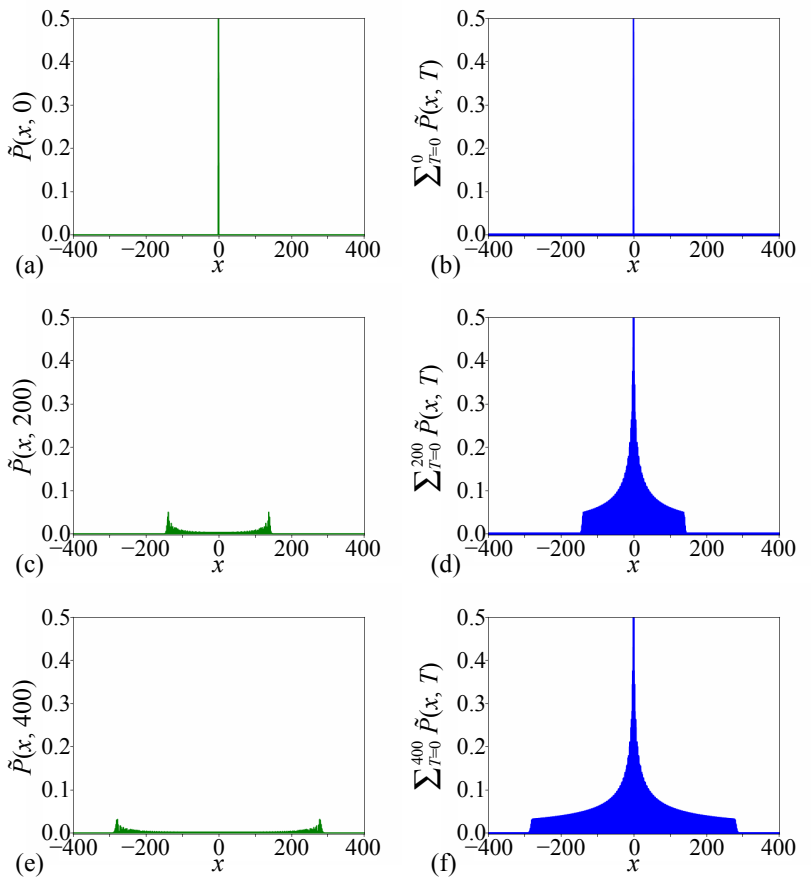

FIG. S1: A numerical example of the probability distribution [(a), (c), (e)] and the temporal sum of the probability [(b), (d), (f)] of the quantum walker after 0 [(a), (b)], 200 [(c), (d)] and 400 [(e), (f)] time steps of evolution in one dimension under the initial condition (S4).

B. Two-dimensional quantum walks

A consistent definition of two-dimensional quantum walks was introduced in Ref. [2]. It starts with the identification of the one-dimensional Dirac Hamiltonian

$$H_{\mathrm{D}}^{(1)} = cp_x\sigma^z + m_x\sigma^y \tag{S6}$$

as an approximate generator of the one-dimensional quantum walk [3], where p_x is the momentum operator in the x direction, m_x is a mass term, and σ^z and σ^y are the Pauli matrices that represent the inner degree of freedom of the Dirac particle. The Trotter decomposition of dynamics due to the Dirac Hamiltonian (S6) yields the dynamics (S5), where the light speed c is proportional to the lattice constant and m_x is proportional to θ in equation (S3).

In squaring the Dirac Hamiltonian (S6), we note that the crossing term disappear because the Pauli matrices are elements of the two-dimensional Clifford algebra: $\sigma^z\sigma^y + \sigma^y\sigma^z = 0$. This motivates us to introduce [2] the Dirac Hamiltonian in two spatial dimensions in the form

$$H_{\mathrm{D}}^{(2)} = (cp_x\sigma^z + m_x\sigma^y) \otimes \tau^0 + \sigma^z \otimes (cp_y\tau^z + m_y\tau^y), \tag{S7}$$

where p_y is the momentum operator in the y direction, m_y is an additional mass term, and τ^z and τ^y are the Pauli matrices in an additional inner degree of freedom with τ^0 being the 2×2 identity matrix in the additional space. In squaring the newly introduced Dirac Hamiltonian (S7) in two spatial dimensions, we note that all crossing terms disappear because the four operators $\sigma^z \otimes \tau^0$, $\sigma^y \otimes \tau^0$, $\sigma^x \otimes \tau^z$ and $\sigma^x \otimes \tau^y$ are elements of the four-dimensional Clifford algebra. The Trotter decomposition of the dynamics due to the Dirac Hamiltonian (S7) yields a consistent definition of quantum walk in two spatial dimensions [2]. It is now straightforward to extend the quantum walk to three and higher-dimensional ones.

S-II. LACK OF ORTHONORMALITY IN NON-HERMITIAN HAMILTONIANS

We here show that in spite of the fact that the pseudo-energy eigenvalues are all fixed to real values, because of the lack of orthonormality of the eigenvectors, the probability and the energy expectation value generally oscillate in time, as we stress at the end of the section defining the one-dimensional model in the main text.

Let us consider a general non-Hermitian Hamiltonian H with $H^\dagger \neq H$. Its eigenvectors are defined in the following manner:

$$\begin{cases} H\left|\psi_n^{\mathrm{R}}\right\rangle = E_n\left|\psi_n^{\mathrm{R}}\right\rangle & \text{for a right-eigenvector } \left|\psi_n^{\mathrm{R}}\right\rangle, \\ \left\langle\psi_n^{\mathrm{L}}\right| H = \left\langle\psi_n^{\mathrm{L}}\right| E_n & \text{for a left-eigenvector } \left\langle\psi_n^{\mathrm{L}}\right|. \end{cases} \tag{S8}$$

Note that the latter is often represented in the form

$$H^\dagger\left|\psi_n^{\mathrm{L}}\right\rangle = {E_n}^*\left|\psi_n^{\mathrm{L}}\right\rangle, \tag{S9}$$

where $\left|\psi_n^{\mathrm{L}}\right\rangle := \left\langle\psi_n^{\mathrm{L}}\right|^\dagger$. In other words, the right- and left- eigenvectors of a non-Hermitian matrix H are essentially the right-eigenvectors of H and $H^\dagger$, respectively. With the definition (S8), the eigenvectors satisfy bi-orthonormality

$$\left\langle\psi_n^{\mathrm{L}}\middle|\psi_m^{\mathrm{R}}\right\rangle = \delta_{nm} \tag{S10}$$

under proper normalization, but the orthonormality is not in general satisfied:

$$\left\langle\psi_n^{\mathrm{R}}\middle|\psi_m^{\mathrm{R}}\right\rangle \neq \delta_{nm}, \tag{S11}$$

where $\left\langle\psi_n^{\mathrm{R}}\right| := \left|\psi_n^{\mathrm{R}}\right\rangle^\dagger$.

Let us specifically look at our non-Hermitian Hamiltonian $H_{\mathrm{NH}}^{(1)}(g)$ in equation (3) as an example. As shown in equation (5), we can make the non-Hermitian matrix $H_{\mathrm{NH}}(g)$ Hermitian with the imaginary gauge transformation $A(g)$ [4, 5] with an imaginary vector potential g. Let $|\psi_n\rangle$ denote the eigenvector for the Hermitian Hamiltonian $H_{\mathrm{NH}}(g=0)$:

$$H_{\mathrm{NH}}(g=0)\left|\psi_n\right\rangle = E_n\left|\psi_n\right\rangle, \tag{S12}$$

$$\left\langle\psi_n\right| H_{\mathrm{NH}}(g=0) = \left\langle\psi_n\right| E_n. \tag{S13}$$

Note that in this case of the Hermitian Hamiltonian $H_{\mathrm{NH}}(g=0)$, the left-eigenvector $\langle\psi_n|$ and the Hermitian conjugate of the right-eigenvector $|\psi_n\rangle$ are the same as in $|\psi_n\rangle = \langle\psi_n|^\dagger$ and the eigenvectors satisfy the standard orthonormality

$$\langle\psi_n|\psi_m\rangle = \delta_{nm}. \tag{S14}$$

From Eqs. (5) and (S12), we obtain the following:

$$A(g)^{-1}H_{\mathrm{NH}}(g)A(g)\left|\psi_n\right\rangle = E_n\left|\psi_n\right\rangle. \tag{S15}$$

Operating $A(g)$ from the left on each side of equation (S15) yields

$$H_{\mathrm{NH}}(g)[A(g)\left|\psi_n\right\rangle] = E_n[A(g)\left|\psi_n\right\rangle]. \tag{S16}$$

We thereby notice that if we take $\left|\psi_n^{\mathrm{R}}\right\rangle$ as in

$$\left|\psi_n^{\mathrm{R}}\right\rangle = A(g)\left|\psi_n\right\rangle, \tag{S17}$$

then equation (S16) is in the completely same form as the top line of equation (S8). Similarly, from Eqs. (5) and (S13), we obtain

$$[\left\langle\psi_n\right| A(g)^{-1}]H_{\mathrm{NH}}(g) = [\left\langle\psi_n\right| A(g)^{-1}]E_n. \tag{S18}$$

Thus we take $\left\langle\psi_n^{\mathrm{L}}\right|$ as in

$$\left\langle\psi_n^{\mathrm{L}}\right| = \left\langle\psi_n\right| A(g)^{-1} \tag{S19}$$

to obtain the bottom line of equation (S8). From Eqs. (S14), (S17) and (S19), we can easily check that the bi-orthonormality (S10) is satisfied while the orthonormality (S11) is not unless $A(g)^\dagger A(g) = \mathbb{I}$, which holds only for $g = 0$ in our case of the non-Hermitian Hamiltonian $H_{\mathrm{NH}}(g)$.

Let us next consider the time evolution of eigenvectors of a general non-Hermitian Hamiltonian H. We assume that the Schrödinger equation for a non-Hermitian Hamiltonian H has the forms

$$\begin{cases} \mathrm{i}\dfrac{\mathrm{d}}{\mathrm{d}t}\left|\psi^{\mathrm{R}}(t)\right\rangle = H\left|\psi^{\mathrm{R}}(t)\right\rangle, \\ -\mathrm{i}\dfrac{\mathrm{d}}{\mathrm{d}t}\left\langle\psi^{\mathrm{L}}(t)\right| = \left\langle\psi^{\mathrm{L}}(t)\right| H, \end{cases} \tag{S20}$$

where we put $\hbar$ to unity. The latter equation may look more plausible in the form

$$\mathrm{i}\frac{\mathrm{d}}{\mathrm{d}t}\left|\psi^{\mathrm{L}}(t)\right\rangle = H^{\dagger}\left|\psi^{\mathrm{L}}(t)\right\rangle. \tag{S21}$$

In other words, the right- and left-eigenvectors are driven by the non-Hermitian Hamiltonians H and $H^{\dagger}$, respectively. This, combined with equation (S8), results in the time-evolution of the forms

$$\begin{cases} \left|\psi_n^{\mathrm{R}}(T)\right\rangle = \mathrm{e}^{-\mathrm{i}E_n T}\left|\psi_n^{\mathrm{R}}(0)\right\rangle, \\ \left\langle\psi_n^{\mathrm{L}}(T)\right| = \mathrm{e}^{+\mathrm{i}E_n T}\left\langle\psi_n^{\mathrm{L}}(0)\right|, \end{cases} \tag{S22}$$

which keeps the bi-orthonormality (S10) intact for any T. Thus if we calculate the probability density with the left- and right-eigenvectors, it does not depend on time:

$$\left\langle\psi^{\mathrm{L}}(T)\middle|\psi^{\mathrm{R}}(T)\right\rangle = \sum_{n,m} {c_m}^* c_n \mathrm{e}^{\mathrm{i}(E_m - E_n)T}\left\langle\psi_m^{\mathrm{L}}\middle|\psi_n^{\mathrm{R}}\right\rangle = \sum_n |c_n|^2, \tag{S23}$$

where we expanded the initial states as

$$\begin{cases} \left|\psi^{\mathrm{R}}(0)\right\rangle = \sum_n c_n \left|\psi_n^{\mathrm{R}}\right\rangle, \\ \left\langle\psi^{\mathrm{L}}(0)\right| = \sum_m {c_m}^* \left\langle\psi_m^{\mathrm{L}}\right|. \end{cases} \tag{S24}$$

The energy expectation value defined in the form $\left\langle\psi^{\mathrm{L}}(T)\middle|H\middle|\psi^{\mathrm{R}}(T)\right\rangle$ is conserved because

$$\left\langle\psi^{\mathrm{L}}(T)\middle|H\middle|\psi^{\mathrm{R}}(T)\right\rangle = \sum_{n,m} {c_m}^* c_n \mathrm{e}^{\mathrm{i}(E_m - E_n)T}\left\langle\psi_m^{\mathrm{L}}\middle|H\middle|\psi_n^{\mathrm{R}}\right\rangle = \sum_n |c_n|^2 E_n. \tag{S25}$$

On the other hand, if we calculate the probability density with the right-eigenvectors and their Hermitian conjugate, then it fluctuates depending on time as follows:

$$\left\langle\psi^{\mathrm{R}}(T)\middle|\psi^{\mathrm{R}}(T)\right\rangle = \sum_{n,m} {c_m}^* c_n \mathrm{e}^{\mathrm{i}({E_m}^* - E_n)T}\left\langle\psi_m^{\mathrm{R}}\middle|\psi_n^{\mathrm{R}}\right\rangle, \tag{S26}$$

whose last factor is not reduced to δ_{mn} because of the inequality (S11). Note that since the imaginary gauge transformation $A(g) = \mathrm{diag}(\mathrm{e}^{-g/2}, \mathrm{e}^{-g/2}, \mathrm{e}^{+g/2}, \mathrm{e}^{+g/2})$ for our model is Hermitian, we have $A(g)^{\dagger}A(g) = A(g)^2 \neq \mathbb{I}$, and hence specifically

$$\left\langle\psi_m^{\mathrm{R}}\middle|\psi_n^{\mathrm{R}}\right\rangle = \langle\psi_m|A(g)^2|\psi_n\rangle \neq \delta_{mn} \tag{S27}$$

unless $g = 0$. Similarly, we can check that the energy expectation value defined in the form $\left\langle\psi^{\mathrm{R}}(T)\middle|H\middle|\psi^{\mathrm{R}}(T)\right\rangle$ is not conserved because

$$\left\langle\psi^{\mathrm{R}}(T)\middle|H\middle|\psi^{\mathrm{R}}(T)\right\rangle = \sum_{n,m} {c_m}^* c_n \mathrm{e}^{\mathrm{i}({E_m}^* - E_n)T}\left\langle\psi_m^{\mathrm{R}}\middle|H\middle|\psi_n^{\mathrm{R}}\right\rangle = \sum_{n,m} {c_m}^* c_n \mathrm{e}^{\mathrm{i}({E_m}^* - E_n)T} E_n \left\langle\psi_m^{\mathrm{R}}\middle|\psi_n^{\mathrm{R}}\right\rangle. \tag{S28}$$

The reason why we use in the present paper the right-eigenvectors and their Hermitian conjugate is because our model is an open quantum system. There are two ways of understanding non-Hermitian systems; one is the closed non-Hermitian system and the other is the open quantum system [6, 7]. The original concept of the PT-symmetric non-Hermitian system [8, 9] was to replace the Hermiticity with more physical symmetries in making certain that the expectation values of the energy and other physical observables are real. Since the system is considered to be closed in this framework, we should employ the right- and left-eigenvectors to keep the bi-orthogonality (S10) satisfied and to make the energy expectation value constant in time as in equation (S25).

The open quantum system, on the other hand, is considered to be embedded in an environment and the entire system of the central system combined with the environment is supposedly Hermitian. Therefore, we should employ the standard way of calculating the expectation value of an observable, if it is localized in the central system or not, by employing the right-eigenvectors and their Hermitian conjugate as in equation (S28). Since the open quantum system can exchange the probability and the energy with the environment, it is natural that the probability density and the energy expectation value are not constant in time (cf. [10, 11]).

S-III. PEAK VELOCITY OF THE QUANTUM WALKERS

We here present the derivation of the peak velocity of quantum walkers, which we used in the analyses of Fig. 3. Consider first the case without the operator $N(g)$, for which the walkers in the ground and excited states are independent of each other. We can then derive the peak velocity as follows. For brevity, let us drop the suffices G and E for the moment and put $\hbar = a = 1$, so that x is an integer.

The walker in each state evolves in time according to the following shift and coin operators:

$$\tilde{S} := \sum_x \left[|x-1\rangle\langle x| \otimes \begin{pmatrix} 1 & 0 \\ 0 & 0 \end{pmatrix} + |x+1\rangle\langle x| \otimes \begin{pmatrix} 0 & 0 \\ 0 & 1 \end{pmatrix} \right], \quad \tilde{C} := \sum_x \left[|x\rangle\langle x| \otimes \begin{pmatrix} \cos\theta & -\sin\theta \\ \sin\theta & \cos\theta \end{pmatrix} \right], \tag{S29}$$

where we represent the inner degree of freedom of two states $|\mathrm{L}\rangle$ and $|\mathrm{R}\rangle$ in Eqs. (S1)–(S3) in terms of 2×2 matrices and we put the lattice constant a to unity. In order to analyze the dynamics efficiently, let us introduce the Fourier transformation in the following forms:

$$|x\rangle = \frac{1}{\sqrt{2\pi}} \int_{-\pi}^{\pi} e^{-\mathrm{i}kx} |k\rangle \, \mathrm{d}k, \quad |k\rangle = \frac{1}{\sqrt{2\pi}} \sum_{x=-\infty}^{\infty} e^{\mathrm{i}kx} |x\rangle \, . \tag{S30}$$

It casts the shift and coin operators into the forms

$$\tilde{S} = \int_{-\pi}^{\pi} \mathrm{d}k \, |k\rangle\langle k| \otimes \begin{pmatrix} \mathrm{e}^{\mathrm{i}k} & 0 \\ 0 & \mathrm{e}^{-\mathrm{i}k} \end{pmatrix}, \quad \tilde{C} = \int_{-\pi}^{\pi} \mathrm{d}k \, |k\rangle\langle k| \otimes \begin{pmatrix} \cos\theta & -\sin\theta \\ \sin\theta & \cos\theta \end{pmatrix}. \tag{S31}$$

We are now in a position to analyze each subspace of k separately. The two eigenvalues of

$$\begin{pmatrix} \mathrm{e}^{\mathrm{i}k} & 0 \\ 0 & \mathrm{e}^{-\mathrm{i}k} \end{pmatrix} \begin{pmatrix} \cos\theta & -\sin\theta \\ \sin\theta & \cos\theta \end{pmatrix} \tag{S32}$$

are given in the form of

$$\lambda_{\pm}(k) := \cos k \cos\theta \pm \mathrm{i}\sqrt{1 - \cos^2 k \cos^2\theta} \tag{S33}$$

or

$$\lambda_{\pm}(k) = \mathrm{e}^{\pm \mathrm{i}E(k)} \tag{S34}$$

with the relation [12]

$$\cos E(k) = \cos k \cos\theta. \tag{S35}$$

The last relation gives the dispersion relation of the quantum walk. The group velocity is then given by

$$v_{\mathrm{g}}(k) := \frac{\mathrm{d}E}{\mathrm{d}k} = \frac{\sin k}{\sin E(k)} \cos\theta. \tag{S36}$$

Its maximum with respect to k should give the peak velocity of the quantum walk because the peaks are the front runners. By further differentiating equation (S36), we have

$$\frac{\mathrm{d}v_{\mathrm{g}}}{\mathrm{d}k} = \left(\frac{\cos k}{\sin E} - \frac{\sin k \cos E \times v_{\mathrm{g}}}{\sin^2 E} \right) \cos\theta = \frac{\cos k}{\sin^3 E} \sin^2\theta \cos\theta. \tag{S37}$$

This thereby shows that the component of $k = \pi/2$ runs fastest and its group velocity gives the peak velocity of the free random walker. Since equation (S35) produces $\cos E(k) = 0$ and $\sin E(k) = \pm 1$ at $k = \pi/2$, the peak velocity of the free random walker is $v_{\mathrm{g}}(\pi/2) = \cos\theta$. We used this fact when we fixed as $\cos\theta_{\mathrm{g}} \simeq 0.270$ and $\cos\theta_{\mathrm{e}} \simeq 0.698$ from Fig. 3 in the main text.

When we have a finite operator $N(g)$, which connects the ground and excited states, we should move over to the 4×4 matrices, again in the Fourier space:

$$C_k := \begin{pmatrix} \cos\theta_{\mathrm{g}} & -\sin\theta_{\mathrm{g}} & & \\ \sin\theta_{\mathrm{g}} & \cos\theta_{\mathrm{g}} & & \\ & & \cos\theta_{\mathrm{e}} & -\sin\theta_{\mathrm{e}} \\ & & \sin\theta_{\mathrm{e}} & \cos\theta_{\mathrm{e}} \end{pmatrix}, \tag{S38}$$

$$S_k := \begin{pmatrix} \mathrm{e}^{\mathrm{i}k} & & & \\ & \mathrm{e}^{-\mathrm{i}k} & & \\ & & \mathrm{e}^{\mathrm{i}k} & \\ & & & \mathrm{e}^{-\mathrm{i}k} \end{pmatrix}, \tag{S39}$$

$$N_k(g) := \exp\left[-\mathrm{i}\begin{pmatrix} -\varepsilon & & -w\mathrm{e}^{-g} & \\ & -\varepsilon & & -w\mathrm{e}^{-g} \\ -w\mathrm{e}^{+g} & & \varepsilon & \\ & -w\mathrm{e}^{+g} & & \varepsilon \end{pmatrix}\right] = \begin{pmatrix} \xi - \mathrm{i}\varepsilon\eta & & \mathrm{i}w\mathrm{e}^{-g}\eta & \\ & \xi - \mathrm{i}\varepsilon\eta & & \mathrm{i}w\mathrm{e}^{-g}\eta \\ \mathrm{i}w\mathrm{e}^{+g}\eta & & \xi + \mathrm{i}\varepsilon\eta & \\ & \mathrm{i}w\mathrm{e}^{+g}\eta & & \xi + \mathrm{i}\varepsilon\eta \end{pmatrix}, \tag{S40}$$

where

$$\xi := \cos\sqrt{\varepsilon^2 + w^2}, \quad \eta := \frac{\sin\sqrt{\varepsilon^2 + w^2}}{\sqrt{\varepsilon^2 + w^2}}. \tag{S41}$$

We thereby numerically find the four eigenvalues of $\mathrm{i}\ln S_k C_k N_k(g)$ in the case of equation (15) as in Fig. S2(a) and compute the group velocity according to each eigenvalue as in Fig. S2(b). For $\epsilon = w = 0$, the red and green curves as well as the orange and blue curves in Fig. S2 would be degenerate. Introduction of finite values of w and ϵ lift the degeneracy; now the green and blue curves are for the ground state, while the red and orange curves are for the excited states. We can indeed observe that the corresponding group velocity for the excited state is greater than the one for the ground state for all k except for $k = 0$ and $k = \pi$. This numerically confirms the expectation that the quantum walker runs faster in the excited state than in the ground state.

For the specific parameter values of equation (15), the maximum of each group velocity gives about ± 0.343 at $k \simeq 0.624\pi$ and ± 0.642 at $k \simeq 0.450\pi$ as indicated by arrows in the figure, which we quoted in the analyses of Fig. 3.

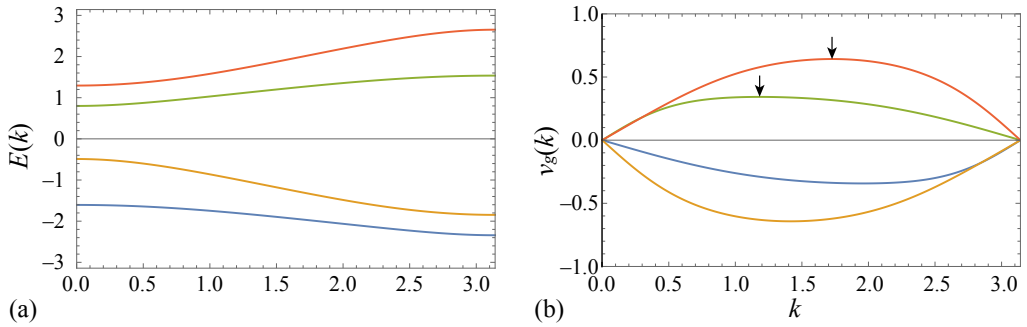

FIG. S2: (a) The k-dependence of the four energy eigenvalues; in other words, the dispersion relation. (b) The k-dependence of the group velocity. The arrows indicate the maxima of the group velocities for the first and second largest eigenvalues. The parameter values are the ones specified in equation (15). We do not show the values for $-\pi < k < 0$ because the dispersion relation is symmetric with respect to $k = 0$ and the group velocity is π-periodic.

S-IV. PROBABILITY OSCILLATIONS BETWEEN THE GROUND AND EXCITED STATES

Here we explain that our active quantum walk is approximately described by an effective two-level Hamiltonian. The description is consistent with the oscillations found in Fig. 4.

We notice in Fig. S2(a), or equivalently in Fig. S3(c) that the upper two levels are the closest to each other at $k = 0$, and symmetrically, the lower two levels at $k = \pi$. We thereby approximately derive an effective Hamiltonian for each set of two levels and show that resonant oscillations between the two levels at the minimum energy gap is quantitively consistent with the oscillation that we find in Fig. 4. We also show an amplification of the probability in the excited level by the factor of e^{2g}, which is also consistent with equation (10).

As shown in Fig. S3(a), the ground and excited states are degenerate for $\varepsilon = w = 0$, for which the upper and lower blocks of C_k in equation (S38) are equal to each other and $N_k(g)$ in equation (S40) is reduced to the identity operator. When we turn on ε to 0.25 but keep $w = 0$ as in Fig. S3(b), the degeneracy between the ground and excited states are lifted except for $k = 0$ for the upper levels and $k = \pi$ for the lower levels. When we further turn on w to 0.25 as in Fig. S3(c), the degeneracies at $k = 0$ and $k = \pi$ are both lifted. We claim that this smallest energy gaps cause the oscillations found in Fig. 4.

Let us here focus on the energy gap at $k = 0$ between the upper two levels, and estimate it by perturbation theory up to the first order of w, keeping ε finite. For $k = 0$, the shift operator (S39) is reduced to the identity operator, and hence irrelevant. The

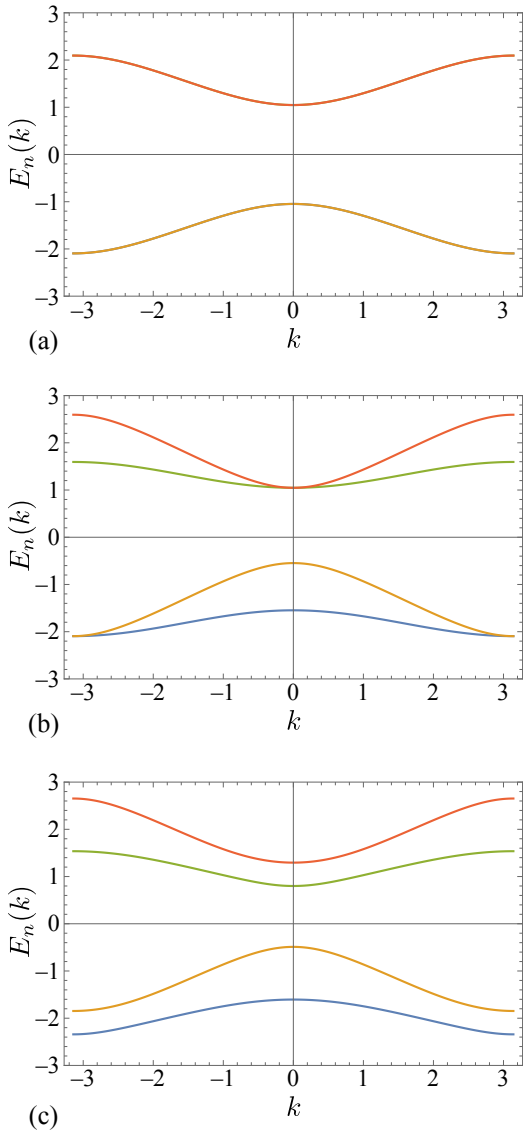

FIG. S3: The dispersion relation of the four pseudo-energy eigenvalues for (a) $\varepsilon = w = 0$, (b) $\varepsilon = 0.25$ with $w = 0$, and (c) $\varepsilon = w = 0.25$. In Panel (a), two curves are degenerate in each of the two curves. Panel (c) is equivalent to Fig. S2(a) but in a doubled plotting region. In all cases, we set $\theta_0 = \pi/3$.

coin operator (S39) keeps the same form. For the operator (S40), the unperturbed limit yields

$$N_g^{(0)} = \begin{pmatrix} \mathrm{e}^{\mathrm{i}\varepsilon} & & & \\ & \mathrm{e}^{\mathrm{i}\varepsilon} & & \\ & & \mathrm{e}^{-\mathrm{i}\varepsilon} & \\ & & & \mathrm{e}^{-\mathrm{i}\varepsilon} \end{pmatrix}, \tag{S42}$$

whereas the first-order perturbation is given by

$$N_g^{(1)} = \mathrm{i}w\eta_0 \begin{pmatrix} & & \mathrm{e}^{-g} & \\ & & & \mathrm{e}^{-g} \\ \mathrm{e}^{+g} & & & \\ & \mathrm{e}^{+g} & & \end{pmatrix} \tag{S43}$$

with $\eta_0 = \sin(\varepsilon)/\varepsilon$. The perturbation parameter w in ξ and η of equation (C16) only contributes to the second-order perturbation, which we neglect hereafter. (Do not confuse the superscripts $^{(0)}$ and $^{(1)}$, which denote in the present Appendix the order of the perturbation, with the same superscripts in the main text, which there denote the dimensionality of the quantum walk.)

To summarize, the unperturbed time-evolution operator for $k = 0$ is

$$\begin{aligned} U_0^{(0)} &:= C_0 N_g^{(0)} \\ &= \begin{pmatrix} \mathrm{e}^{\mathrm{i}\varepsilon} \begin{pmatrix} \cos\theta_\mathrm{g} & -\sin\theta_\mathrm{g} \\ \sin\theta_\mathrm{g} & \cos\theta_\mathrm{g} \end{pmatrix} & \\ & \mathrm{e}^{-\mathrm{i}\varepsilon} \begin{pmatrix} \cos\theta_\mathrm{e} & -\sin\theta_\mathrm{e} \\ \sin\theta_\mathrm{e} & \cos\theta_\mathrm{e} \end{pmatrix} \end{pmatrix} = \begin{pmatrix} \mathrm{e}^{-\mathrm{i}(\theta_g\sigma_y-\varepsilon)} & \\ & \mathrm{e}^{-\mathrm{i}(\theta_e\sigma_y+\varepsilon)} \end{pmatrix}, \end{aligned} \tag{S44}$$

while the first-order perturbation is given by

$$U_0^{(1)} := C_0 N_g^{(1)} = \mathrm{i}w\eta_0 \begin{pmatrix} & \mathrm{e}^{-g} \begin{pmatrix} \cos\theta_\mathrm{g} & -\sin\theta_\mathrm{g} \\ \sin\theta_\mathrm{g} & \cos\theta_\mathrm{g} \end{pmatrix} \\ \mathrm{e}^{+g} \begin{pmatrix} \cos\theta_\mathrm{e} & -\sin\theta_\mathrm{e} \\ \sin\theta_\mathrm{e} & \cos\theta_\mathrm{e} \end{pmatrix} & \end{pmatrix}. \tag{S45}$$

The unperturbed eigenvectors that diagonalize the unperturbed matrix (S45) are

$$\left|\psi_{\mathrm{g}+}^{(0)}\right\rangle = \frac{1}{\sqrt{2}}\begin{pmatrix}1\\ \mathrm{i}\\ 0\\ 0\end{pmatrix}, \quad \left|\psi_{\mathrm{e}+}^{(0)}\right\rangle = \frac{1}{\sqrt{2}}\begin{pmatrix}0\\ 0\\ 1\\ \mathrm{i}\end{pmatrix}, \quad \left|\psi_{\mathrm{g}-}^{(0)}\right\rangle = \frac{1}{\sqrt{2}}\begin{pmatrix}1\\ -\mathrm{i}\\ 0\\ 0\end{pmatrix}, \quad \left|\psi_{\mathrm{e}-}^{(0)}\right\rangle = \frac{1}{\sqrt{2}}\begin{pmatrix}0\\ 0\\ 1\\ -\mathrm{i}\end{pmatrix}, \tag{S46}$$

which give the unperturbed eigenvalues as

$$\lambda_{\mathrm{g}+}^{(0)} = \mathrm{e}^{-\mathrm{i}(\theta_\mathrm{g}-\varepsilon)} = \mathrm{e}^{-\mathrm{i}\theta_0}, \quad \lambda_{\mathrm{e}+}^{(0)} = \mathrm{e}^{-\mathrm{i}(\theta_\mathrm{e}+\varepsilon)} = \mathrm{e}^{-\mathrm{i}\theta_0}, \quad \lambda_{\mathrm{g}-}^{(0)} = \mathrm{e}^{-\mathrm{i}(-\theta_\mathrm{g}-\varepsilon)}, \quad \lambda_{\mathrm{e}-}^{(0)} = \mathrm{e}^{-\mathrm{i}(-\theta_\mathrm{e}+\varepsilon)}. \tag{S47}$$

The eigenvalues $\lambda_{\mathrm{g}+}^{(0)}$ and $\lambda_{\mathrm{e}+}^{(0)}$ in equation (S47) correspond to the positive pseudo-energies, which are degenerate to θ_0 as in the upper two levels of Fig. S3(b). (The eigenvalues $\lambda_{\mathrm{g}-}^{(0)}$ and $\lambda_{\mathrm{e}-}^{(0)}$ are degenerate to the negative pseudo-energy $-\theta_0$ at $k = \pi$ rather than $k = 0$.)

In other words, the unperturbed eigenvectors in equation (S46) both give the same eigenvalue $\mathrm{e}^{-\mathrm{i}\theta_0}$. We therefore diagonalized the following matrix to find the first-order perturbed eigenvalues:

$$\Delta U = \begin{pmatrix} \left\langle\psi_{\mathrm{g}+}^{(0)}\right| U_0^{(1)} \left|\psi_{\mathrm{g}+}^{(0)}\right\rangle & \left\langle\psi_{\mathrm{g}+}^{(0)}\right| U_0^{(1)} \left|\psi_{\mathrm{e}+}^{(0)}\right\rangle \\ \left\langle\psi_{\mathrm{e}+}^{(0)}\right| U_0^{(1)} \left|\psi_{\mathrm{g}+}^{(0)}\right\rangle & \left\langle\psi_{\mathrm{e}+}^{(0)}\right| U_0^{(1)} \left|\psi_{\mathrm{e}+}^{(0)}\right\rangle \end{pmatrix}. \tag{S48}$$

Straightforward algebra produces

$$\Delta U = \mathrm{i}w\eta_0 \mathrm{e}^{-\mathrm{i}\theta_0} \begin{pmatrix} 0 & \mathrm{e}^{-g-\mathrm{i}\varepsilon} \\ \mathrm{e}^{+g+\mathrm{i}\varepsilon} & 0 \end{pmatrix}. \tag{S49}$$

Since the eigenvalues of the matrix above are ± 1, we have the eigenvalues up to the first order of w in the form

$$\lambda_\pm \simeq \mathrm{e}^{-\mathrm{i}\theta_0} \left(1 \pm \mathrm{i}w\eta_0\right). \tag{S50}$$

The pseudo-energy eigenvalues are thereby given by

$$E_\pm := \mathrm{i}\log\lambda_\pm \simeq \theta_0 \mp w\eta_0. \tag{S51}$$

Therefore, the energy gap at $k = 0$ is found to be $\Delta E = 2w\eta_0$. For $\varepsilon = 0.25$ and $w = 0.25$, we have $\Delta E \simeq 0.494808$. The period of the oscillation is $2\pi/\Delta E \simeq 12.6982$, which is consistent with the oscillation found in Fig. 4.

Let us finally find the effective Hamiltonian that governs the dynamics in the Hilbert subspace of the two vectors in equation (S46). The matrix

$$V := \begin{pmatrix} 1 & \mathrm{e}^{-g-\mathrm{i}\varepsilon} \\ \mathrm{e}^{+g+\mathrm{i}\varepsilon} & -1 \end{pmatrix} \tag{S52}$$

diagonalizes ΔU with

$$V^{-1} = \frac{1}{-2}\begin{pmatrix} -1 & -\mathrm{e}^{-g-\mathrm{i}\varepsilon} \\ -\mathrm{e}^{+g+\mathrm{i}\varepsilon} & 1 \end{pmatrix} = \frac{V}{2} \tag{S53}$$

as in $V^{-1}\Delta U V = \mathrm{diag}\,(\lambda_+, \lambda_-)$. This implies that the effective Hamiltonian is given by

$$H_{\text{eff}} := V \begin{pmatrix} E_+ & \\ & E_- \end{pmatrix} V^{-1} = \begin{pmatrix} \theta_0 & -w\eta_0 \mathrm{e}^{-g-\mathrm{i}\varepsilon} \\ -w\eta_0 \mathrm{e}^{+g+\mathrm{i}\varepsilon} & \theta_0 \end{pmatrix}. \tag{S54}$$

The effective time-evolution operator within this Hilbert subspace is therefore found to be

$${U_{\text{eff}}}^T := \mathrm{e}^{-\mathrm{i}H_{\text{eff}}T} = \mathrm{e}^{-\mathrm{i}\theta_0 T} \exp\left[\mathrm{i}w\eta_0 T \begin{pmatrix} 0 & \mathrm{e}^{-g-\mathrm{i}\varepsilon} \\ \mathrm{e}^{+g+\mathrm{i}\varepsilon} & 0 \end{pmatrix}\right] \tag{S55}$$

In calculating the matrix exponential above, we take full advantage of a complex version of the gauge transformation in equation (5). Using the gauge transformation

$$A(g+\mathrm{i}\varepsilon) = \begin{pmatrix} \mathrm{e}^{-(g+\mathrm{i}\varepsilon)/2} & 0 \\ 0 & \mathrm{e}^{+(g+\mathrm{i}\varepsilon)/2} \end{pmatrix}, \tag{S56}$$

we have

$$A^{-1} \begin{pmatrix} 0 & \mathrm{e}^{-g-\mathrm{i}\varepsilon} \\ \mathrm{e}^{+g+\mathrm{i}\varepsilon} & 0 \end{pmatrix} A = \begin{pmatrix} 0 & 1 \\ 1 & 0 \end{pmatrix}. \tag{S57}$$

We therefore find

$$\exp\left[\mathrm{i}w\eta_0 T \begin{pmatrix} 0 & \mathrm{e}^{-g-\mathrm{i}\varepsilon} \\ \mathrm{e}^{+g+\mathrm{i}\varepsilon} & 0 \end{pmatrix}\right] = A \begin{pmatrix} \cos(w\eta_0 T) & \mathrm{i}\sin(w\eta_0 T) \\ \mathrm{i}\sin(w\eta_0 T) & \cos(w\eta_0 T) \end{pmatrix} A^{-1} = \begin{pmatrix} \cos(w\eta_0 T) & \mathrm{i}\mathrm{e}^{-g-\mathrm{i}\varepsilon}\sin(w\eta_0 T) \\ \mathrm{i}\mathrm{e}^{+g+\mathrm{i}\varepsilon}\sin(w\eta_0 T) & \cos(w\eta_0 T) \end{pmatrix} \tag{S58}$$

Suppose, for example, that we start the time evolution from $\left|\psi^{(0)}_{\mathrm{g}+}\right\rangle$. We thereby find

$$|\psi_+(T)\rangle := {U_{\text{eff}}}^T \left|\psi^{(0)}_{\mathrm{g}+}\right\rangle = e^{-\mathrm{i}\theta_0 T} \begin{pmatrix} \cos(w\eta_0 T) \\ \mathrm{i}\mathrm{e}^{+g+\mathrm{i}\varepsilon}\sin(w\eta_0 T) \end{pmatrix} \tag{S59}$$

Therefore the following probabilities for the ground and excited states oscillate as in

$$P_{\mathrm{g}}(T) := \left| \left\langle \psi^{(0)}_{\mathrm{g}+} \middle| {U_{\text{eff}}}^T \middle| \psi^{(0)}_{\mathrm{g}+} \right\rangle \right|^2 = \cos^2(w\eta_0 T), \tag{S60}$$

$$P_{\mathrm{e}}(T) := \left| \left\langle \psi^{(0)}_{\mathrm{e}+} \middle| {U_{\text{eff}}}^T \middle| \psi^{(0)}_{\mathrm{g}+} \right\rangle \right|^2 = \mathrm{e}^{2g}\sin^2(w\eta_0 T); \tag{S61}$$

see Fig. S4. For $g = 0$, this simply describes the resonant oscillation between the ground and excited states with the probability conservation $P_{\mathrm{g}}(T) + P_{\mathrm{e}}(T) = 1$. For $g > 0$, we find the enhancement of the oscillation amplitude of the excited state by the factor of e^{2g}, which is consistent with equation (10). The oscillation should describe the behavior that we observe in Fig. 4.

For $w = 0$ as in Fig. S4(a), the ground and excited states of the effective Hamiltonian are degenerate and we do not observe any difference or oscillation between the two states. This corresponds to the case of Fig. 4(a). As we introduce the off-diagonal elements of N_g to be $w = 0.25$, the oscillation of the phase difference of π for the ground and excited states appears with the period $\pi/(w\eta_0) \simeq 12.6982$ for $\varepsilon = 0.25$, or about 8 oscillations in the range $0 \le T \le 100$, which is consistent with what we observe in Fig. 4(b). We notice nonetheless that the value for the sum of the two states (green line) constantly increases without any oscillations in Fig. 4(b). This corresponds to the probability conservation $P_{\mathrm{g}}(T) + P_{\mathrm{e}}(T) = 1$. Finally, when we introduce g as in Fig. 4(c) and (d), we see that the green curve now oscillates with the same phase as the value for the excited state. This implies that the oscillation amplitude of the excited state is enhanced by the factor e^{2g}, which is consistent with the observation in equation (S61).

[1] Y. Aharonov, L. Davidovich, and N. Zagury. Quantum random walks. *Phys. Rev. A*, 48:1687–1690, Aug 1993.

[2] Manami Yamagishi, Naomichi Hatano, Ken-Ichiro Imura, and Hideaki Obuse. Proposal of multidimensional quantum walks to explore Dirac and Schrödinger systems. *Phys. Rev. A*, 107:042206, Apr 2023.

[3] Frederick W. Strauch. Relativistic quantum walks. *Phys. Rev. A*, 73:054302, May 2006.

[4] Naomichi Hatano and David R. Nelson. Localization Transitions in Non-Hermitian Quantum Mechanics. *Phys. Rev. Lett.*, 77:570–573, Jul 1996.

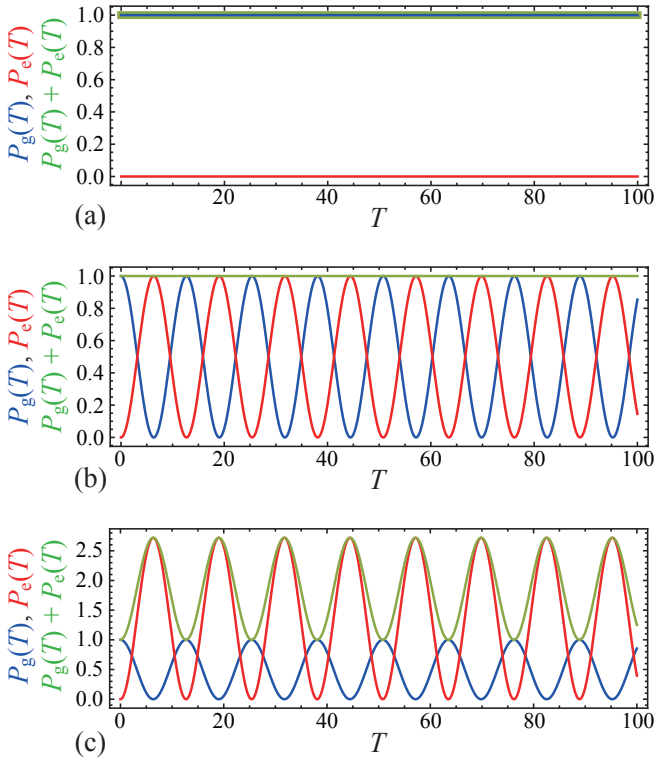

FIG. S4: The oscillation of the probabilities in Eqs. (S60) and (S61). In each panel, the horizontal axis indicates t, the blue curve indicates $P_{\rm g}(t)$, the red curve indicates $P_{\rm e}(t)$, and the green curve indicates the summation. (a) $w = 0$ and $g = 0$. (b) $w = 0.25$ and $g = 0$. (c) $w = 0.25$ and $g = 0.5$.

[5] Naomichi Hatano and David R. Nelson. Vortex pinning and non-Hermitian quantum mechanics. *Phys. Rev. B*, 56:8651–8673, Oct 1997.

[6] Kohei Kawabata. Private communication. Comment on the use of the left-eigenvector and the Hermitian conjugate of the right-eigenvector., December 2018.

[7] Naomichi Hatano. What is the resonant state in open quantum systems? *Journal of Physics: Conference Series*, 2038(1):012013, oct 2021.

[8] Carl M. Bender and Stefan Boettcher. Real Spectra in Non-Hermitian Hamiltonians Having PT Symmetry. *Phys. Rev. Lett.*, 80:5243–5246, Jun 1998.

[9] Carl M. Bender, Dorje C. Brody, and Hugh F. Jones. Complex Extension of Quantum Mechanics. *Phys. Rev. Lett.*, 89:270401, Dec 2002.

[10] K. G. Makris, R. El-Ganainy, D. N. Christodoulides, and Z. H. Musslimani. Beam Dynamics in $\mathcal{PT}$ Symmetric Optical Lattices. *Phys. Rev. Lett.*, 100:103904, Mar 2008.

[11] Christian E Rüter, Konstantinos G Makris, Ramy El-Ganainy, Demetrios N Christodoulides, Mordechai Segev, and Detlef Kip. Observation of parity–time symmetry in optics. *Nat. Phys.*, 6(3):192–195, March 2010.

[12] A. Kempf and R. Portugal. Group velocity of discrete-time quantum walks. *Phys. Rev. A*, 79:052317, May 2009.